Advances in Geo-Energy Research

Vol. 7, No. 1, p. 66-68, 2023

Research highlight

Understanding hydraulic fracture mechanisms: From the laboratory to numerical modelling

Aly Abdelaziz, Johnson Ha, Mei Li, Earl Magsipoc, Lei Sun*, Giovanni Grasselli

Department of Civil and Mineral Engineering, University of Toronto, Toronto M5S 1A4, Canada

Keywords:
Hydraulic fracturing
true triaxial
fracture classification
serial section reconstruction
dual-porosity model

Cited as:
Abdelaziz, A., Ha, J., Li, M., Magsipoc, E., Sun, L., Grasselli, G. Understanding hydraulic fracture mechanisms: From the laboratory to numerical modelling. Advances in Geo-Energy Research, 2023, 7(1): 66-68.
https://doi.org/10.46690/ager.2023.01.07

Abstract:
The development of fracture networks associated with hydraulic fracturing operations are extremely complex multiphysics processes and there is still no accepted methodology for mapping or realistic recreating such fracture networks. This is an issue especially for modeling purposes, as, ideally, an accurate numerical representation, and subsequent numerical model, should be able to honor the trajectory, type, connectivity, and geometric properties of the complex fracture network generated. This research proposes a novel framework capable of conducting fluid flow numerical simulations based on mapped fracture networks induced during hydraulic fracturing laboratory experiments where a shale sample, under true triaxial reservoir stress conditions, is subjected to fluid injection to mimic a single stage open-hole in-situ hydraulic fracture operation. The resulting post-test fracture network of the shale sample is filled with fluorescent dyed epoxy and subsequently imaged. The images are segmented, and individual fractures are classified based on their geometrical characteristics, as parted bedding planes, opened natural fractures, and newly generated hydraulic fractures. The digital fracture network is numerically represented for fluid flow simulation using a dual-porosity model within the finite volume method. In the numerical reconstruction, fractures are implicitly represented in a set of cells with virtual fracture aperture. The properties of each grid cell are assigned based on fracture classification, and flow between grid cells is explicitly assigned based on the connectivity of the grid cells. Findings show faster fluid drainage parallel to bedding planes (horizontal) than in the vertical direction, indicating strong fluid flow anisotropy.

Accounting for discontinuities, imperfections, anisotropy planes is essential in understanding the dynamics behind reservoir fracturing, and hence, is key to understand the performance of any underground operation related to the energy sector, such as geothermal energy, hydraulic fracturing operations, carbon capture and storage (Tsang and Neretnieks, 1998). It is accepted that the interaction between pre-existing natural fractures and those hydraulically induced has a pronounced role in dictating the fracture trajectory and thus the geometry of the stimulated rock volume (Zhao et al., 2016; Feng et al., 2020; Al Mteiri et al., 2021). During hydraulic fracturing of shale formations, the general belief within the energy sector is that bi-wing fractures develop and propagate perpendicular to the least principal stress (σ_3) (Hubbert and Willis, 1957) and, by connecting to natural fractures, form a complex fracture network from where hydrocarbon is recovered. However, this "dogma" downplays the effect finely laminated bedding planes, characterized by significantly weaker frictional and tensile strengths, have on the rocks failure process (Shimamoto and Logan, 1981). This work contributes to better understand the influence of such interactions and their overall impact on reservoir performance, including but not limited to, fluid production of the stimulated rock volumes.

Difficulties representing fracture interactions arise either due to limitations in capturing the geometrical features, extent, and connectivity of fractures, or to the use of equivalent mathematical representations (e.g., stochastic) that do not honor the complexity of the fracture network (Liu et al., 2022). In this work, a framework capable of numerically simulating an actual fracture network, while honoring its

Yandy Scientific Press

*Corresponding author.
E-mail address: aly.abdelaziz@mail.utoronto.ca (A. Abdelaziz); johnson.ha@utoronto.ca (J. Ha); meili.li@mail.utoronto.ca (M. Li); e.magsipoc@mail.utoronto.ca (E. Magsipoc); leo.sun@mail.utoronto.ca (L. Sun); giovanni.grasselli@utoronto.ca (G. Grasselli).

Received August 26, 2022; revised September 17, 2022; accepted September 27, 2022; available online October 1, 2022.

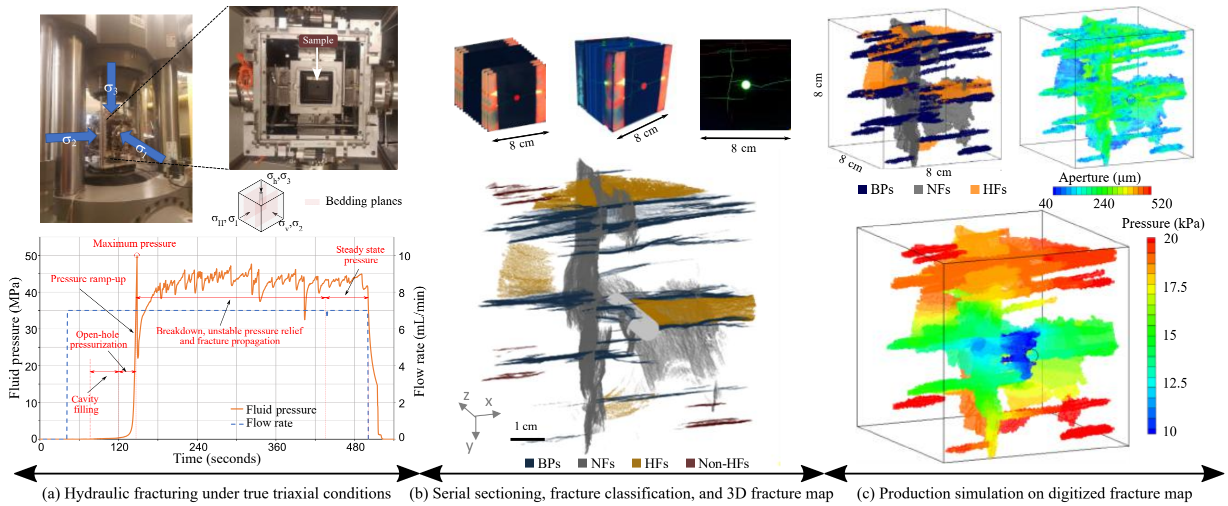

Fig. 1. The framework showing the various phases. (a) The first phase shows the true triaxial hydraulic fracturing setup, the sample being tested, and a typical schematic of a hydraulic pressure curve obtained from the experiment (Abdelaziz et al., 2019), (b) the second phase shows the serial sectioning process from stacking, registration, and segmentation to obtain the 3D fracture map (modified from Li et al., 2022), (c) the third phase shows the reconstructed and digitized 3D fracture map (top-left) classifying the different types of fractures, the aperture representation of the fracture map (top-right), and the resulting fluid pressure distribution (bottom) using the dual-porosity model within the finite volume method. BPs: bedding planes, NFs: natural fractures, HFs: newly generated hydraulic fractures.

complexity, geometrical features, extent, and connectivity is proposed. The framework comprises three main phases that are conducted sequentially. First, a laboratory-scale fracture network is hydraulically induced in a rock sample under in-situ reservoir true triaxial stress conditions. Then, the resulting fracture network from the laboratory experiment is digitized to quantify and categorize the various components that constitute the induced fracture network (Magsipoc et al., 2020; Li et al., 2022). Finally, the categorized fracture network is numerically reconstructed and utilized to simulate fluid production within the fractured rock mass using a dual-porosity model within the finite volume method.

The three-dimensional (3D) volume of the 80 mm × 80 mm × 80 mm shale rock sample is scanned using a micro-computed tomography (μCT) machine at a resolution of 110 μm to assess the pre-existing condition of the rock. The shale rock sample is then inserted into the true triaxial laboratory testing equipment (Lombos et al., 2012; Young et al., 2012). The experiment is performed in a controlled environment replicating reservoir in-situ stresses and fluid injection pressures. Fluid is injected through a 6 mm diameter mini-well, drilled along the σ_3 direction to the center of the cube, which mimics a single stage open-hole in-situ hydraulic fracture operation (Abdelaziz et al., 2019). The laboratory test concludes shortly after reaching a steady-state pressure after the hydraulic breakdown pressure (Figure 1(a)). The hydraulically failed sample is then impregnated with fluorescent dyed epoxy to fill the fracture network and establish a strong visual contrast between the fractures and the rock matrix (Figure 1(b)). A surface grinding machine is used to sequentially remove a 50 μm thick layer per grinding cycle from the post-test sample, perpendicular to the mini-well. After each cycle, the surface is photographed under ultraviolet light, to collect serial section images and build a digital 3D map of the rock sample at a resolution of 39 μm × 39 μm × 50 μm. The resulting image stack has a high intensity contrast between the rock matrix and the epoxy-illuminated fractures. To assess the fracture type, the connectivity to the injection mini-well, orientation, dip angle, and surface roughness, characterized by the directional roughness metric (Tatone and Grasselli, 2009), as well as pre-existing fractures, identified from the initial μCT scan, are taken into consideration. The assessment classifies the fractures into hydraulically connected fractures and non-hydraulic fractures, with the latter having no connectivity to the injection mini-well. The hydraulically connected fractures are further classified into parted bedding planes, natural fractures, and newly generated hydraulic fractures. In addition, the fracture trace and aperture of each fracture is determined, which inherently establishes the interconnectivity, in terms of flow, between the various fractures. These fracture parameters allow for the numerical simulation to honor the spatial distribution of the fractures, their interconnectivity, as well as their geometrically derived hydraulic properties (i.e., aperture). The numerical model is built on a pixel level reconstruction of the digital 3D fracture network. Grids that intersect fracture pixels are defined as fracture elements, while the remaining grids are defined as matrix elements. The fracture elements are labelled according to their classification and are assigned their respective aperture value. Fracture elements that belong to more than one fracture trace form channels and are assigned agglomerated hydraulic properties representative of their connectivity at the pixel level. In doing so, the anisotropic fluid flow in a fracture element is adequately captured even when intersected by multiple fractures. The numerical model is then run to assess the fluid flow within the fractured rock using a dual-porosity approach combined with the finite volume method. This approach enables fluid flow in both the fracture network and rock matrix with distinct permeabilities, as well as the flux exchange between fractures and rock matrix.

Laboratory post-test visual observation of the shale rock sample studied herein revealed that the dominant fracture propagation path was along the bedding plane. The digital fracture network, obtained after serial sectioning, further confirmed those preliminary observations indicating the key role played by bedding planes in creating the fracture network. Quantitative analysis of the digitally reconstructed fracture network shows that the hydraulically connected fractures accounted for about 97% of the total fracture volume present in the tested sample, partitioned into 62% bedding planes, 30% pre-existing opened natural fractures, and 5% newly generated hydraulic fractures (Li et al., 2022). In addition, directional roughness analysis highlights that the natural fractures are rougher compared to the bedding planes, that might result in more tortuous flow paths and lower fluid transmissivity.

The experimentally generated fracture network exhibits complex interactions between existing fractures, bedding planes, and newly generated hydraulic fractures. Incorporating such findings into a dual-porosity numerical model provides insights on the contribution of each fracture to the overall reservoir performance. Since the numerical parameters within the dual-porosity model honor the spatial distribution, characteristics, and aperture of all fractures, the simulation results show strong fluid flow anisotropy within the fracture network, confirming that this fracture geometry favors horizontal fluid drainage versus the expected vertical direction. It is also capable of correctly replicating the spatial distribution, interconnectivity, and geometrically derived hydraulic properties of the fracture within the numerical simulation. The simulation results clearly highlight the importance of fracture apertures, spatial distribution, and distance of the fractures with respect to the injection mini-well (Figure 1(c)). Finally, although the framework here details a laboratory-scale hydraulic fracturing experiment, the framework is robust and can be applied to any type of fracture network.

Acknowledgements

This work was supported by the Natural Sciences and Engineering Research Council of Canada (NSERC) Discovery (Nos. 341275, PGS D3-518886) and NSERC/Energi Simulation Industrial Research Chair.

Conflict of interest

The authors declare no competing interest.

References

Abdelaziz, A., Ha, J., Abul Khair, H., et al. Unconventional shale hydraulic fracturing under true triaxial laboratory conditions, the value of understanding your reservoir. Paper SPE 196026 Presented at SPE Annual Technical Conference and Exhibition, Calgary, Alberta, Canada, 30 September-2 October, 2019.

Al Mteiri, S., Suboyin, A., Rahman, M. M., et al. Hydraulic fracture propagation and analysis in heterogeneous middle eastern tight gas reservoirs: Influence of natural fractures and well placement. ACS Omega, 2021, 6(1): 799-815.

Feng, Q., Xu, S., Xing, X., et al. Advances and challenges in shale oil development: A critical review. Advances in Geo-Energy Research, 2020, 4(4): 406-418.

Hubbert, M. K., Willis, D. G. Mechanics of hydraulic fracturing. Transactions of the AIME, 1957, 210(1): 153-168.

Li, M., Magsipoc, E., Abdelaziz, A., et al. Mapping fracture complexity of fractured shale in laboratory: Three-dimensional reconstruction from serial-section images. Rock Mechanics and Rock Engineering, 2022, 55(5): 2937-2948.

Liu, C., Zhang, L., Li, Y., et al. Effects of microfractures on permeability in carbonate rocks based on digital core technology. Advances in Geo-Energy Research, 2022, 6(1): 86-90.

Lombos, L., Roberts, D. W., King, M. S. Design and development of integrated true triaxial rock testing system. True Triaxial Testing of Rocks, 2012, 4: 35.

Magsipoc, E., Li, M., Abdelaziz, A., et al. Analysis of the fracture morphologies from a laboratory hydraulic fracture experiment on Montney shale. Paper ARMA-IGS-20-061 Presented at ARMA/DGS/SEG International Geomechanics Symposium, Virtual, 3-5 November, 2020.

Shimamoto, T., Logan, J. M. Effects of simulated clay gouges on the sliding behavior of Tennessee sandstone. Tectonophysics, 1981, 75(3-4): 243-255.

Tatone, B. S. A., Grasselli, G. A method to evaluate the three-dimensional roughness of fracture surfaces in brittle geomaterials. Review of Scientific Instruments, 2009, 80(12): 125110.

Tsang, C. F., Neretnieks, I. Flow channeling in heterogeneous fractured rocks. Reviews of Geophysics, 1998: 36(2): 275-298.

Young, R. P., Nasseri, M. H.B., Lombos, L. Imaging the effect of the intermediate principal stress on strength, deformation and transport properties of rocks using seismic methods, in True Triaxial Testing of Rocks, edited by Kwasniewski, M., Li, X., and Takahashi, M., CRC Press, London, pp. 167-179, 2012.

Zhao, Z., Li, X., Wang, Y., et al. A laboratory study of the effects of interbeds on hydraulic fracture propagation in shale formation. Energies, 2016, 9(7): 556.